

This is the peer reviewed version of the following article:

Bader, C. and Sorvina, A. and Simpson, P. and Wright, P. and Stagni, S. and Plush, S. and Massi, M. et al. 2016. Imaging nuclear, endoplasmic reticulum, and plasma membrane events in real time. FEBS Letters.,

which has been published in final form at <http://doi.org/10.1002/1873-3468.12365>

This article may be used for non-commercial purposes in accordance with Wiley Terms and Conditions for Self-Archiving at <http://olabout.wiley.com/WileyCDA/Section/id-820227.html#terms>

# 1 **Imaging nuclear, endoplasmic reticulum and plasma membrane events in** 2 **real time**

3 Christie A. Bader<sup>1</sup>, Alexandra Sorvina<sup>1</sup>, Peter V. Simpson<sup>2</sup>, Phillip J. Wright<sup>2</sup>, Stefano  
4 Stagni<sup>3</sup>, Sally E. Plush<sup>1</sup>, Massimiliano Massi<sup>2</sup>, Douglas A. Brooks<sup>1\*</sup>

5 <sup>1</sup>Mechanisms in Cell Biology and Disease Research Group, School of Pharmacy and Medical  
6 Sciences, Sansom Institute for Health Research, University of South Australia, Adelaide,  
7 Australia.

8 <sup>2</sup>Department of Chemistry and Nanochemistry Research Institute, Curtin University, Bentley,  
9 Australia.

10 <sup>3</sup>Department of Industrial Chemistry “Toso Montanari”, University of Bologna, Bologna,  
11 Italy.

12

## 13 **Abstract**

14 Live cell imaging can provide important information on cellular dynamics, however the full  
15 utilisation of this technology has been hampered by the limitation imaging reagents. Metal-  
16 based complexes have the potential to overcome many of the issues common to many current  
17 imaging agents. The rhenium (I) based complex *fac*-[Re(CO)<sub>3</sub>(1,10-phenanthroline)(4-  
18 pyridyltetrazolate)], herein referred to as ReZolve-ER<sup>TM</sup>, shows promise as a live cell  
19 imaging agent with rapid cell uptake, low cytotoxicity, resistance to photobleaching and  
20 compatibility with multicolour imaging. ReZolve-ER<sup>TM</sup> localised to the nuclear  
21 membrane/endoplasmic reticulum (ER) and allowed the detection of exocytotic events at the  
22 plasma membrane. Thus, we present a new imaging agent for monitoring live cell events in  
23 real time, which is ideal for imaging either short or long time courses.

24

## 25 **Introduction**

26 One of the most exciting advances in cell biology has been the development of technology  
27 for live cell imaging, which enables the visualisation of molecular events in real time.  
28 However, while there have been significant advances in spatial and temporal resolution  
29 imaging, with for example spinning disk, fast scanning and super resolution microscope  
30 technologies [1,2], the field of imaging reagents has struggled to keep pace. This is partially  
31 because the imaging reagent market is undergoing a quantum shift from imaging reagents  
32 that require cell fixation, which is known to generate significant artefacts [3], to those that  
33 enable real time live cell imaging. Reagents for live cell imaging ideally should exhibit *in situ*  
34 stability, optimal emission/photophysical properties, a large Stokes shift, resistance to  
35 photobleaching, capacity for multicolour/multiple probe imaging and most importantly low  
36 toxicity [4]. Consequently, there is a very high demand for imaging reagents that meet these  
37 criteria to enable effective live cell imaging without perturbing cellular mechanisms.

38

39 There are a range of technical approaches for live cell imaging, including endogenous  
40 fluorescence, genetic expression systems, quantum dots and small fluorescent molecules.

41 Endogenous fluorescence has been effectively used for *in vitro* live cell and *intravital*  
42 imaging [5,6], and while this mode of imaging does not require exogenous labelling there are  
43 only a limited number of molecules capable of generating detectable endogenous  
44 fluorescence [7]. Furthermore, endogenous fluorescence (often referred to as  
45 autofluorescence) can actually be a hindrance when combined with specific microscopy  
46 imaging techniques [8]. While GFP expression systems revolutionised the field of  
47 mammalian cell biology [9,10], this technology requires genetic manipulation of the target.  
48 Moreover, the GFP molecule is large and can cause steric problems that influence molecular  
49 function [11]. In addition, many molecular targets, including carbohydrates and lipids are not  
50 amenable to this technology. While the use of quantum dot imaging is rapidly increasing, this  
51 nanocrystal technology can be prone to particle breakdown, toxicity and high production  
52 costs [12]. To date the majority of the commercially available reagents for fluorescence  
53 imaging have been based on organic compounds, like BODIPY. These compounds can suffer  
54 from a range of issues including concentration dependent fluorescent shifts, photobleaching  
55 and cytotoxicity. To address the growing need for specific, high quality imaging reagents that  
56 do not affect cell viability, researchers have been exploring luminescent metal complexes,  
57 such as those of Re(I), Ru(II), Ir(III), Pt(II) and the trivalent lanthanides [13-16]. Metal  
58 complexes have the potential to overcome a number of the pitfalls associated with organic  
59 fluorophores, as they are typically resistant to photobleaching, allowing excitation for longer  
60 periods of times with respect to organic fluorophores. Moreover, the triplet multiplicity  
61 nature of the excited states of these species implies that their excited state lifetime is usually  
62 elongated, ranging between hundreds of nanoseconds to milliseconds depending on the  
63 structure of the complex. Compared to the fast decay of endogenous autofluorescence, the  
64 transition metal characteristics can be exploited in time-gated imaging techniques, to  
65 improve signal-to-noise ratios. Lastly, the large Stokes shift of luminescent metal  
66 complexes is beneficial to avoid issues with concentration dependent quenching.

67

68 Recently, we have shown that the Re(I) complex *fac*-[Re(CO)<sub>3</sub>(**phen**)(L<sup>3py</sup>)], where **phen** is  
69 1,10-phenanthroline and L<sup>3py</sup> is 3-pyridyltetrazolate can be utilised for live cell imaging, and  
70 it localises to acidic vesicles [17]. This complex was also found to be highly resistant to  
71 photobleaching, strongly emissive with a large Stokes shifts and long emission life times,  
72 whilst exhibiting minimal to no cytotoxicity [17]. We have also shown that changes to the  
73 tetrazolate structure result in changes in intracellular distribution, whilst retaining the key  
74 properties for live cell imaging (photobleaching resistant, large Stokes shift, minimal  
75 cytotoxicity). For example the exchange of the L<sup>3py</sup> for 4-cyanophenyltetrazolate results in  
76 Re(I) complex (ReZolve-L1<sup>TM</sup>) with shown preferential localisation within the lipid droplet  
77 [17,18]. Therefore, in the interest of designing new Re(I) complexes for cell imaging, we  
78 furthered our investigation of altering the chemical nature of the ancillary ligand to highlight  
79 consequent effects in biological behaviour of the metal-based complex. We have previously  
80 published the synthesis, electrochemical and photophysical properties of the analogous Re(I)  
81 complex bound to the 4-pyridyltetrazolate ligand, herein designated as ReZolve-ER<sup>TM</sup> [19].  
82 Remarkably, preliminary investigation into the incubation and localisation of this complex  
83 revealed a different staining pattern with respect to *fac*-[Re(CO)<sub>3</sub>(**phen**)(L<sup>3py</sup>)], despite the  
84 only difference between the two complexes being the 3- or 4-pyridyl substituent. Intrigued by  
85 this initial finding we continued our investigation and here we show that ReZolve-ER<sup>TM</sup>

86 localises to the endoplasmic reticulum (ER) [17]. Furthermore we show that ReZolve-ER<sup>TM</sup>  
87 is ideal for live cell imaging applications, with rapid detection within cells, resistance to  
88 photobleaching, consistent cellular localisation and low cytotoxicity. In addition, ReZolve-  
89 ER<sup>TM</sup> allowed the visualisation of specific nuclear events, ER structures and vesicle release  
90 from the cell surface, demonstrating that this compound is suitable for investigating a range  
91 of biological questions related to cellular dynamics.

92

## 93 **Materials and Methods**

### 94 **Cell culture and staining**

95 The non-malignant cell lines PNT1a and PNT2 and prostate cancer cell line LNCaP (clone  
96 FCG) were obtained from the European Collection of Cell Cultures via CellBank Australia  
97 (Children's Medical Research Institute, NSW, Australia). Prostate cancer cell line DU145,  
98 was obtained from the American Tissue Culture Collection via Cryosite (Cryosite Ltd., New  
99 South Wales, Australia). Chinese hamster ovaries CHO-K1 cell line and Human monocytic  
100 leukemia THP-1 cell line were obtained from the American Type Culture Collection via  
101 Sigma-Aldrich (Sigma-Aldrich, St. Louis, USA).

102

103 The PNT1a, PNT2, CHO-K1 and THP-1 cell lines were maintained in Roswell Park  
104 Memorial Institute (RPMI) 1640 culture medium (Sigma-Aldrich, USA), supplemented with  
105 10% foetal calf serum (In Vitro Technologies, Australia), 2 mM L-glutamine (Sigma-Aldrich,  
106 USA). The DU-145 cell line was cultured in minimum essential medium (Gibco, Life  
107 Technologies, USA), supplemented with 10% foetal calf serum, 2 mM L-glutamine and 1  
108 mM sodium pyruvate (Sigma-Aldrich, USA). The LNCaP cell line was cultured in RPMI-  
109 1640 media (Gibco, Life Technologies, USA) supplemented with 2 mM L-glutamine, 10 %  
110 FCS, 10 mM HEPES (Sigma-Aldrich, USA) and 1 mM sodium pyruvate. THP-1 monocytes  
111 were differentiated into macrophages by incubation with RPMI-1640 medium containing 5  
112 ng/mL of phorbol 12-myristate 13-acetate (Sigma-Aldrich, USA) over 48 hours. Cells were  
113 cultured to approximately 90% confluence before passage, by washing with sterile PBS  
114 (Sigma-Aldrich, St. Louis, USA), TrypLE<sup>TM</sup> Express (Gibco, USA) to dissociate the cells  
115 from the culture surface and then resuspended in supplemented culture medium. Cell lines  
116 were maintained at 37°C and 5% CO<sub>2</sub> in a Sanyo MCO-17AI humidified incubator (Sanyo  
117 Electric Biomedical, Japan). For imaging experiment cells were culture in Ibidi  $\mu$ -slides 8  
118 wells (Ibidi, Germany) and for MTS assays PNT2 cells were cultured in 96 well plates.

119

120 For cellular imaging, cells were incubated with 50  $\mu$ M ReZolve-ER<sup>TM</sup> prepared in serum free  
121 cell culture media, from a 10 mM stock solution prepared in DMSO. Cells were then imaged  
122 immediately or following 15 min of incubation without washing cells. For co-staining  
123 experiments cell were stained with ER-Tracker<sup>®</sup> Red, MitoTracker<sup>®</sup> Red CMXRos,  
124 LysoTracker<sup>®</sup> Red DND-99 or CellMask<sup>TM</sup> (Molecular Probes, USA), according to the  
125 manufactures instructions. Cells were then washed 2 x 30 sec in PBS. Serum free media  
126 containing 50 $\mu$ M of ReZolve-ER<sup>TM</sup> was then added and images were collected after 15  
127 minutes of incubation. Cell fixation was performed using 4% paraformaldehyde in PBS for

128 20 minutes at room temperature. Cells were then washed for 3 x 10 minutes in PBS before  
129 incubation with 50  $\mu$ M ReZolve-ER<sup>TM</sup> for 20 minutes.

130

### 131 **Confocal imaging and analysis**

132 For confocal imaging cells were held in a Uno-Combined-Controller, CO<sub>2</sub> microscope  
133 electric top stage incubation system (Okolab, Italy) held at 37°C and 5% CO<sub>2</sub>. Confocal  
134 imaging was performed on a Nikon A1<sup>+</sup> confocal microscope, fitted with a LU-N4/LU-N4S  
135 4-laser unit (405 nm, 488 nm, 561 nm, 640 nm), the A1-DUG GaAsP Multi Detector Unit (2  
136 GaAsP PMTs + 2 standard PMTs) and a 32 channel spectral detector (Nikon, Japan). Images  
137 were captured using a 60x oil emersion lens. Each confocal micrograph represented 0.5  $\mu$ m  
138 thin optical sections.

139

140 To assess emission intensity of ReZolve-ER<sup>TM</sup> over time NIS-Elements software (Nikon,  
141 Japan) was used. Regions of interest were selected using the AutoDetect function to select  
142 cells containing ReZolve-ER<sup>TM</sup>, mean emission intensity was then measured over time for  
143 each region of interest. For each experiment greater than six regions of interest were used to  
144 gain the average emission intensity in Microsoft Excel 2013 (which were then plotted against  
145 time). Co-localisation between ReZolve-ER<sup>TM</sup> and ER-Tracker® Red, MitoTracker® Red  
146 CMXRos or LysoTracker® Red DND-99 was assessed in NIS-Elements software (Nikon,  
147 Japan) using the co-localisation analysis to generate a Pearson's correlation coefficient. Cells  
148 from a minimum of 10 images for each marker were measured for co-localisation and the  
149 means were compared by ANOVA analysis in GraphPad Prism with Tukey post-hoc analysis  
150 (Prism software, version 6.01, USA).

### 151 **Cytotoxicity assay**

152 To assess cytotoxicity of the complexes, cellular NAD(P)H-dependent redox activity was  
153 measured using CellTiter 96<sup>®</sup> Aqueous Non-Radioactive Cell Proliferation Assay (MTS)  
154 according to the manufacturer instruction (Promega, USA). Briefly, PNT2 cells were cultured  
155 as described above in 96 well plates for 24 h. Cells were then incubated with 50  $\mu$ M of  
156 ReZolve-ER<sup>TM</sup> for 1 h, 4 h, 8 h or 24 h in serum free media, for a control cells were incubate  
157 with 0.5% v/v DMSO in serum free media for the corresponding incubation time without the  
158 presence of ReZolve-ER<sup>TM</sup>. Media was then removed and replaced by 120  $\mu$ L of MTS and  
159 PMS in RPMI-1640 medium and allowed to incubate at room temperature for 1 h. The  
160 absorbance was then measured at 490 nm by EnSpire Plate Readers (PerkinElmer, USA).

161

### 162 **Results and discussion**

163 The synthesis and photophysical properties of ReZolve-ER<sup>TM</sup> have previously been reported  
164 [19]. This complex was found to be compatible with fluorescent microscopy using single  
165 photon excitation at 403 nm or two-photon excitation between 800 nm and 830 nm, making it  
166 amenable for use with a range of microscopy set ups and applications.

167

168 ***ReZolve-ER<sup>TM</sup> cellular uptake is by passive diffusion.***

169 For effective cellular imaging, reagents need to penetrate the cell membrane and accumulate  
170 in a cell at a high enough concentration for detection by fluorescence microscopy. To assess  
171 this, live non-malignant prostate PNT2 cells were incubated with ReZolve-ER<sup>TM</sup> at 50  $\mu$ M,  
172 and the emission monitored in real time over 30 minutes (Supplementary Video 1). Using a  
173 Nikon A1 microscope (equipped with a live cell incubator), the emission from ReZolve-  
174 ER<sup>TM</sup> was detected within seconds after the complex was applied, using a low excitation  
175 power (403 nm excitation laser set to < 2 power setting) and a low detector sensitivity (Si  
176 PMT HV detector 180). Initially ReZolve-ER<sup>TM</sup> could be detected in the cytoplasm, but  
177 within the first minute of addition, the accumulation of the complex could be detected in the  
178 peri-nuclear region. The emission intensity increased throughout the cell over the first 10  
179 minutes. After this time, the intensity and localisation of the complex appeared to be  
180 consistent for the next 20 minutes of image collection. The ability to detect the complex in  
181 cells within seconds of addition, at low laser power, is important as this will prevent photo-  
182 damage of live cells and suggested the potential for ReZolve-ER<sup>TM</sup> as a real time imaging  
183 agent.

184

185 The rapid entry of ReZolve-ER<sup>TM</sup> into PNT2 cells suggested that this complex was able to  
186 freely transit across the cell membrane. Furthermore, the signal from the ReZolve-ER<sup>TM</sup> was  
187 concentration dependent, and a concentration of 50  $\mu$ M was optimal for imaging, with lower  
188 concentrations resulting in weaker signal detection. When cells that had been labelled with  
189 ReZolve-ER<sup>TM</sup> were washed (i.e. media containing ReZolve-ER<sup>TM</sup> was replaced with fresh  
190 culture medium containing no dye), there was an immediate reduction in the ReZolve-ER<sup>TM</sup>  
191 detection. This suggested that ReZolve-ER<sup>TM</sup> had a low affinity for its cellular target; and  
192 supported the premise that a passive diffusion mechanism was involved for ReZolve-ER<sup>TM</sup>  
193 cell entry, as this mechanism is dependent on a concentration gradient. To further confirm  
194 this mode of entry, cells were fixed in paraformaldehyde and incubated with ReZolve-ER<sup>TM</sup>.  
195 The complex could be easily detected in these cells following fixation, confirming passive  
196 transport as the mode of cell entry (Supplementary figure 1). The rapid uptake of ReZolve-  
197 ER<sup>TM</sup> is ideal for real time imaging of cells and the ability to control the addition or removal  
198 of the complex may be well suited to the long term monitoring of specific cellular structures.

199

200 To assess the photostability of ReZolve-ER<sup>TM</sup> in cells, PNT2 cells were incubated with the  
201 complex and imaged continuously using a higher laser power, in an attempt to induce  
202 photobleaching. Images were collected with a scan rate of 0.22 seconds and a pixel dwell  
203 time of 0.22 milliseconds for a total of 448 scans (approximately 29 minutes), with the  
204 excitation power set to a setting of 10, which was five times greater than the maximum power  
205 required for ReZolve-ER<sup>TM</sup> visualisation. Over the first eight minutes of image collection the  
206 intensity increased as the complex accumulated in cells (Figure 1), as was observed when a  
207 lower laser power was used (Supplementary video 1). Between eight and 29 minutes the  
208 emission intensity remained constant (Figure 1); suggesting that the complex was highly  
209 resistant to photobleaching. However, an increase in emission intensity was observed in the  
210 final minutes of acquisition when using a high laser power (five times the power required for  
211 visualisation), indicating that photo-activation may be occurring.

212

213 ***ReZolve-ER<sup>TM</sup> is detected at the ER and nucleoplasmic reticulum.***

214 In different cell lines, including non-malignant prostate cells (PNT2 and PNT1a), malignant  
215 prostate cancer cells (LNCaP and DU145), CHO-K1 cells and THP-1 macrophages  
216 (Supplementary Figure 2), ReZolve-ER<sup>TM</sup> detected a central structure within the nucleus that  
217 resembled the nucleolus, with projections towards the nuclear membrane; as well as a diffuse  
218 reticular network emanating from the nuclear region, which extended into distal regions of  
219 the cell. To further define this intracellular distribution, ReZolve-ER<sup>TM</sup> was co-stained with  
220 ER-Tracker® (ER), MitoTracker® (mitochondria), LysoTracker® (lysosomes/acidic vesicles)  
221 and CellMask<sup>TM</sup> (plasma membrane) in PNT2 cells. PNT2 cells were labelled with the latter  
222 commercial dyes, the cells were briefly washed and then incubated with 50 µM ReZolve-  
223 ER<sup>TM</sup> for 15 to 20 minutes before imaging (Figure 2). ReZolve-ER<sup>TM</sup> showed significant co-  
224 localisation with ER-Tracker®, with a Pearson's correlation coefficient of  $0.84\pm 0.01$ . Co-  
225 localisation between ReZolve-ER<sup>TM</sup> and ER-Tracker® was observed on the reticular network  
226 extending from the nucleus into the cytoplasm, at the nuclear membrane and on membranous  
227 structures extending into the nucleus that appear to be nucleoplasmic reticulum (Figure 2A).  
228 The nucleoplasmic reticulum has been previously visualised using ER markers, such as ER-  
229 Tracker® [20, 21] or ER associated Ca<sup>2+</sup>-ATPase [22], which was consistent with ReZolve-  
230 ER<sup>TM</sup> detecting a similar, biologically related structure. In contrast, there was only a limited  
231 amount of ReZolve-ER<sup>TM</sup> detected in association with mitochondria (Figure 2B) and  
232 lysosomes (Figure 2C), which was shown by lower Pearson's correlation coefficients for co-  
233 localisation between ReZolve-ER<sup>TM</sup> and either MitoTracker® or LysoTracker® of  $0.44\pm 0.01$   
234 or  $0.37\pm 0.01$ , respectively. While most of the mitochondrial and lysosomal labelling was  
235 independent of ReZolve-ER<sup>TM</sup> some overlap was detected between these structures (Figure  
236 2B, 2C). This overlap between ReZolve-ER<sup>TM</sup> and mitochondria or lysosomes was not  
237 surprising given the close association between the ER and these two subcellular  
238 compartments [23, 24]. Interestingly, while ReZolve-ER<sup>TM</sup> did not stain large areas of the  
239 plasma membrane (Figure 2; i.e. limited co-localisation with CellMask<sup>TM</sup>), there was some  
240 specific sites of co-localization with CellMask<sup>TM</sup> (Figure 5B), which may have identified a  
241 localised interaction between the endoplasmic reticulum and the cell surface.

242 From this co-location study we propose that ReZolve-ER<sup>TM</sup> locates to the ER and  
243 biologically related structures, in live cells. The mechanism by which ReZolve-ER<sup>TM</sup>  
244 associates with the nuclear membrane/ER is not currently known, but a similar tricarbonyl  
245 rhenium(I) diimine luminescent complex, ReZolve-L1<sup>TM</sup>, has been shown to localise with  
246 polar lipids in cells [17, 18]. Given that the ER is a major site of lipid synthesis [25], we can  
247 speculate that ReZolve-ER<sup>TM</sup> may have a similar lipophilic interaction.

248

249 ***ReZolve-ER<sup>TM</sup> remains in ER structures during longer term real time imaging.***

250 For long term imaging experiments it is important for a reagent to be retained in cells over a  
251 long period of time, and to cause minimal to no damage to the cells. PNT2 cells were  
252 incubated with ReZolve-ER<sup>TM</sup> and imaged for 280 minutes at 10 minute intervals to assess  
253 the compatibility of the complex with long term imaging. Over 280 minutes ReZolve-ER<sup>TM</sup>  
254 remained localised to the perinuclear region of cells (Figure 3A-C). Although the intensity of

255 the emission from ReZolve-ER<sup>TM</sup> decreased over time, it was still easily detected at the end  
256 of the time course (Figure 3C, 3D). The decrease in emission intensity was likely due to the  
257 complex being slowly trafficked out of the cell, and not related to photobleaching, as the  
258 complex was photo-resistant and exhibited continuous emission in response to extended laser  
259 exposure (Figure 3). To assess the potential cytotoxic effects of ReZolve-ER<sup>TM</sup>, PNT2 cells  
260 were incubated with the complex for 1, 4, 7 or 24 hours and the cell viability assessed via an  
261 MTS assay (Figure 3E). Cell viability (as indicated by absorbance) was reduced when treated  
262 with ReZolve-ER<sup>TM</sup> at 50  $\mu$ M for 1 hour and 4 hours compared to controls, however the  
263 viability was still significantly higher than the negative control (Figure 3E). Although cell  
264 viability was reduced by this complex, cells imaged with ReZolve-ER<sup>TM</sup> for the 4 hours did  
265 not show morphological changes, which would have indicated cytotoxicity during this time,  
266 thus suggesting that the cytotoxicity of ReZolve-ER<sup>TM</sup> was low. Interestingly, following 7  
267 hours and 24 hours of incubation with ReZolve-ER<sup>TM</sup> the cell viability was unchanged when  
268 compared to controls (Figure 3E). While this may be due to complex efflux, it showed that  
269 long term exposure to the ReZolve-ER<sup>TM</sup> does not affect overall cell survival. The minimal  
270 cytotoxic effects of ReZolve-ER<sup>TM</sup> and its ability to be detected in cells over a long time  
271 periods make this complex an ideal tool for live cell imaging.

272

### 273 ***Detection of nuclear and ER events with ReZolve-ER<sup>TM</sup>.***

274 A number of time series images were collected using ReZolve-ER<sup>TM</sup> (Figures 4 and 5) and  
275 these revealed inward projections from the nuclear membrane, which resembled a phagocytic  
276 event at the nuclear membrane (Figure 4), as well as a number of small vesicles in the cellular  
277 periphery (Figure 5). Figure 4 shows that ReZolve-ER<sup>TM</sup> detected the formation of a large  $\sim$ 3  
278  $\mu$ m nuclear membrane derived phagosome that appeared to sequester part of the nucleoplasm  
279 (Supplementary Video 2). ReZolve-ER<sup>TM</sup> clearly defined the nuclear membrane extension as  
280 well as the phagosome vesicle formation, closure and release event, which was evident  
281 during the 5 minute imaging time course. It is generally accepted that trafficking into and out  
282 of the nucleus occurs through nuclear pores, which is facilitated by the nuclear pore complex  
283 [26], but budding and formation of vesicles can also occur from the nuclear envelope [27-29].  
284 For example, ribonucleoprotein particles can be exported out of the nucleus in a process  
285 similar to viral capsid nuclear egress, where small vesicles have been observed forming at the  
286 nuclear envelop, before budding out to release their content [27]. In TEM images  
287 multivesicular bodies have also been visualised in close proximity to the nuclear envelope  
288 and in some cases these multivesicular structures appeared to be forming from the nuclear  
289 envelope [28,29]. Although the identity of this nuclear structure is unclear, and we cannot  
290 rule out an artificially induced cellular response to the complex, it seemed that ReZolve-  
291 ER<sup>TM</sup> was able to visualise specific nuclear events in real time, indicating its potential for live  
292 cell imaging applications.

293

294 To further explore the detection of small ( $<$  0.5  $\mu$ m) vesicles by ReZolve-ER<sup>TM</sup> in the cellular  
295 periphery, a dual labelling time-course experiment was performed using both ReZolve-ER<sup>TM</sup>  
296 and CellMask<sup>TM</sup>. This enabled the simultaneous visualisation of two distinct vesicular events  
297 at the cell surface (Figure 5; Supplementary Video 3). CellMask<sup>TM</sup> identified a  $\sim$  1  $\mu$ m  
298 diameter vesicle forming over an eight minute time course, involving a membrane protrusion

299 from the cell surface and then vesicle budding/excision from the plasma membrane; and  
300 interestingly this microvesicle contained a small amount of diffuse ReZolve-ER<sup>TM</sup> staining in  
301 its lumen (Figure 5B). The detection of ReZolve-ER<sup>TM</sup> inside the budding vesicle (Figure 5B)  
302 could be consistent with the dissociation of the dye from the membrane into the vesicle (N.B.  
303 cell washing significantly reduced the staining, suggesting that ReZolve-ER<sup>TM</sup> has a low  
304 affinity for its target); however we could not exclude the possibility that ReZolve-ER<sup>TM</sup> was  
305 identifying a specific target within these budding vesicles. In addition, a small (< 0.5 μm)  
306 vesicle with intense ReZolve-ER<sup>TM</sup> staining was visualised: first distorting a specific location  
307 on the plasma membrane and showing co-location with CellMask<sup>TM</sup>; and then pushing  
308 through the plasma membrane to be released from the cell (Figure 5C). This later event  
309 occurred more rapidly (~ 2-3 minutes) when compared to the former 1 μm diameter vesicle  
310 formation and release (~ 8-9 minutes). These observations suggest that ReZolve-ER<sup>TM</sup> has  
311 the potential for not only visualising the ER, but also vesicle trafficking out of the cell.

312

### 313 **Conclusion**

314 Visualising cellular organelles such as the ER can provide powerful insights for  
315 understanding cellular dynamics under a range of physiological conditions. The ER plays a  
316 central role in protein transcription, molecular trafficking and cellular signalling.  
317 Endoplasmic reticulum stress is commonly observed in a range of diseases and in response to  
318 physiological stress, and thus the ability to track the ER over large time periods may provide  
319 new insights into diseases such as cancer, non-alcoholic fatty liver disease, diabetes and  
320 neurodegenerative disease. Thus an imaging reagent such as ReZolve-ER<sup>TM</sup> that can monitor  
321 the ER has potential applications in facilitating our understanding of cell biology in a range  
322 of diseases. Given that ReZolve-ER<sup>TM</sup> has the ability to be used over short or long time  
323 courses, is highly resistant to photobleaching, can be removed from cells, has low  
324 cytotoxicity over long exposure times and has already demonstrated its ability to detect  
325 interesting cellular phenomena in real time, this imaging reagent could be utilised in a  
326 multitude of experimental protocols and provide a flexible imaging tool for cell biologists.

327

### 328 **Acknowledgements.**

329 This work was supported by funding from the University of South Australia, an ITEK  
330 catalyst grant and a BioSA Innovation grant awarded to DAB, SP and MM. MM also wishes  
331 to thank the ARC for funding (FT130100033). The authors declare a financial interest in  
332 ReZolve-ER<sup>TM</sup> as this imaging agent is being commercialized by ReZolve Scientific.

333

### 334 **Author contribution**

335 CB, SP, MM and DB conceived and supervised the study; CB SP and DB designed  
336 experiments; CB and AS performed experiments; PS, PW and SS provided and characterised  
337 new tools and reagents; CB, SP and DB wrote the manuscript; AS, PS, PW, SS and MM  
338 made manuscript revisions.

339

340 References  
341

- 342 1. Nakano A (2002) Spinning-disk confocal microscopy- A cutting-edge tool for imaging of membrane  
343 traffic. *Cell Struct Funct* 27: 349-355.
- 344 2. Hell SW (2009) Microscopy and its focal switch. *Nat Meth* 6: 24-32.
- 345 3. Rastogi V, Puri N, Arora S, Kaur G, Yadav L, et al. (2013) Artefacts: A diagnostic dilemma. *J Clin*  
346 *Diagn Res* 7: 2408-2413.
- 347 4. Ettinger A, Wittmann T (2014) Chapter 5 - Fluorescence live cell imaging. In: Jennifer CW, Torsten  
348 W, editors. *Methods Cell Bio: Academic Press*. pp. 77-94.
- 349 5. Shandala T, Lim C, Sorvina A, Brooks D (2013) A *Drosophila* model to image phagosome  
350 maturation. *Cells* 2: 188.
- 351 6. Zipfel WR, Williams RM, Christie R, Nikitin AY, Hyman BT, et al. (2003) Live tissue intrinsic emission  
352 microscopy using multiphoton-excited native fluorescence and second harmonic generation.  
353 *Proc Natl Acad Sci USA* 100: 7075-7080.
- 354 7. Croce AC, Bottiroli G (2014) Autofluorescence spectroscopy and imaging: A tool for biomedical  
355 research and diagnosis. *Eur J Histochem* 58: 2461.
- 356 8. Yang Y, Honaramooz A (2012) Characterization and quenching of autofluorescence in piglet testis  
357 tissue and cells. *Anat Res Inter*.
- 358 9. Chalfie M, Tu Y, Euskirchen G, Ward WW, Prasher DC (1994) Green fluorescent protein as a  
359 marker for gene expression. *Science* 263: 802-805.
- 360 10. Heim R, Prasher DC, Tsien RY (1994) Wavelength mutations and posttranslational autoxidation of  
361 green fluorescent protein. *Proc Natl Acad Sci USA* 91: 12501-12504.
- 362 11. Kuruppu S, Tochon-Danguy N, Ian Smith A (2013) Applicability of green fluorescence protein in  
363 the study of endothelin converting enzyme-1c trafficking. *Protein Sci* 22: 306-313.
- 364 12. Zhu Z-J, Yeh Y-C, Tang R, Yan B, Tamayo J, et al. (2011) Stability of quantum dots in live cells. *Nat*  
365 *Chem* 3: 963-968.
- 366 13. New EJ, Congreve A, Parker D (2010) Definition of the uptake mechanism and sub-cellular  
367 localisation profile of emissive lanthanide complexes as cellular optical probes. *Chem Sci* 1:  
368 111-118.
- 369 14. Baggaley E, Weinstein JA, Williams JAG (2012) Lighting the way to see inside the live cell with  
370 luminescent transition metal complexes. *Coord Chem Rev* 256: 1762-1785.
- 371 15. Coogan MP, Fernandez-Moreira V (2014) Progress with, and prospects for, metal complexes in  
372 cell imaging. *Chem Commun* 50: 384-399.
- 373 16. Lo KK-W (2015) Luminescent rhenium(I) and iridium(III) polypyridine complexes as biological  
374 probes, imaging reagents, and photocytotoxic Agents. *Acc Chem Res* 48: 2985-2995.
- 375 17. Bader CA, Brooks RD, Ng YS, Sorvina A, Werrett MV, et al. (2014) Modulation of the organelle  
376 specificity in Re( I) tetrazolato complexes leads to labeling of lipid droplets dagger. *RSC Adv*  
377 4: 16345-16351.
- 378 18. Bader CA, Carter EA, Safitri A, Simpson PV, Wright P, et al. (2016) Unprecedented staining of  
379 polar lipids by a luminescent rhenium complex revealed by FTIR microspectroscopy in  
380 adipocytes. *Mol Biosys* 12: 2064-2068.
- 381 19. Wright PJ, Muzzioli S, Werrett MV, Raiteri P, Skelton BW, et al. (2012) Synthesis, photophysical  
382 and electrochemical investigation of dinuclear tetrazolato-bridged rhenium complexes.  
383 *Organometallics* 31: 7566-7578.
- 384 20. Collings DA, Carter CN, Rink JC, Scott AC, Wyatt SE, et al. (2000) Plant nuclei can contain  
385 extensive grooves and invaginations. *Plant Cell* 12: 2425-2440.
- 386 21. Isaac C, Pollard JW, Meier UT (2001) Intranuclear endoplasmic reticulum induced by Nopp140  
387 mimics the nucleolar channel system of human endometrium. *J Cell Sci* 114: 4253-4264.
- 388 22. Collado-Hilly M, Shirvani H, Jaillard D, Mauger JP (2010) Differential redistribution of Ca<sup>2+</sup>-  
389 handling proteins during polarisation of MDCK cells: Effects on Ca<sup>2+</sup> signalling. *Cell Calcium*  
390 48: 215-224.

391 23. Rowland AA, Voeltz GK (2012) Endoplasmic reticulum-mitochondria contacts: function of the  
392 junction. *Nat Rev Mol Cell Biol* 13: 607-625.

393 24. López-Sanjurjo CI, Tovey SC, Prole DL, Taylor CW (2013) Lysosomes shape Ins(1,4,5)P3-evoked  
394 Ca<sup>2+</sup> signals by selectively sequestering Ca<sup>2+</sup> released from the endoplasmic reticulum. *J*  
395 *Cell Sci* 126: 289-300.

396 25. Fagone P, Jackowski S (2009) Membrane phospholipid synthesis and endoplasmic reticulum  
397 function. *J Lipid Res* 50 Suppl: S311-316.

398 26. Mor A, White MA, Fontoura BMA (2014) Nuclear trafficking in health and disease. *Curr Opin Cell*  
399 *Biol* 28: 28-35.

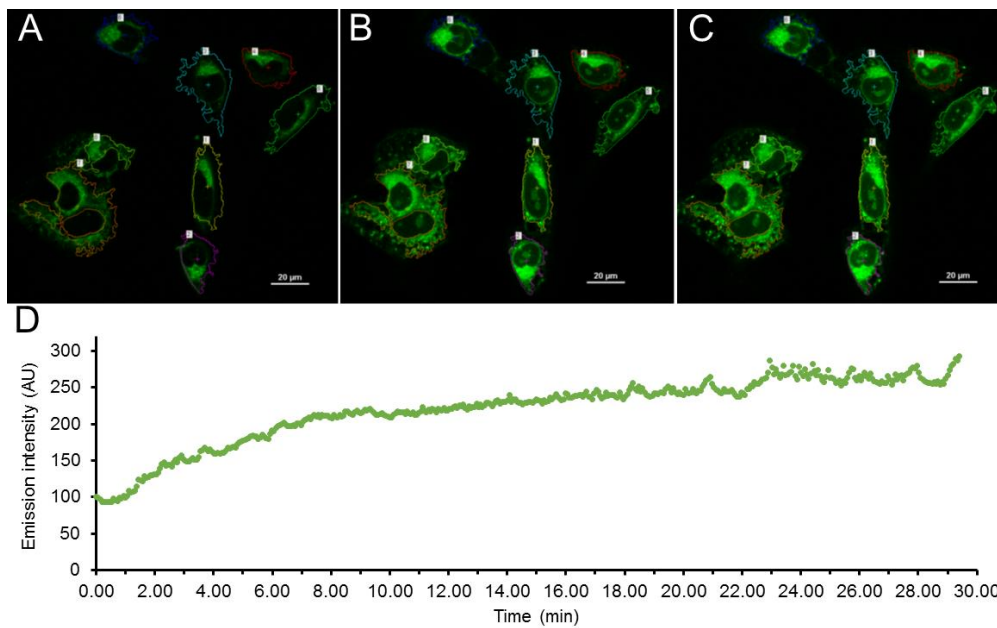
400 27. Speese SD, Ashley J, Jokhi V, Nunnari J, Barria R, et al. (2012) Nuclear envelope budding enables  
401 large ribonucleoprotein particle export during synaptic Wnt signaling. *Cell* 149: 832-846.

402 28. Kilarski W, Jasinski A (1970) The formation of multivesicular bodies from the nuclear envelope. *J*  
403 *Cell Biol* 45: 205-211.

404 29. Majumdar R, Tameh AT, Parent CA (2016) Exosomes mediate LTB4 release during neutrophil  
405 chemotaxis. *PloS Biol* 14: e1002336.

406

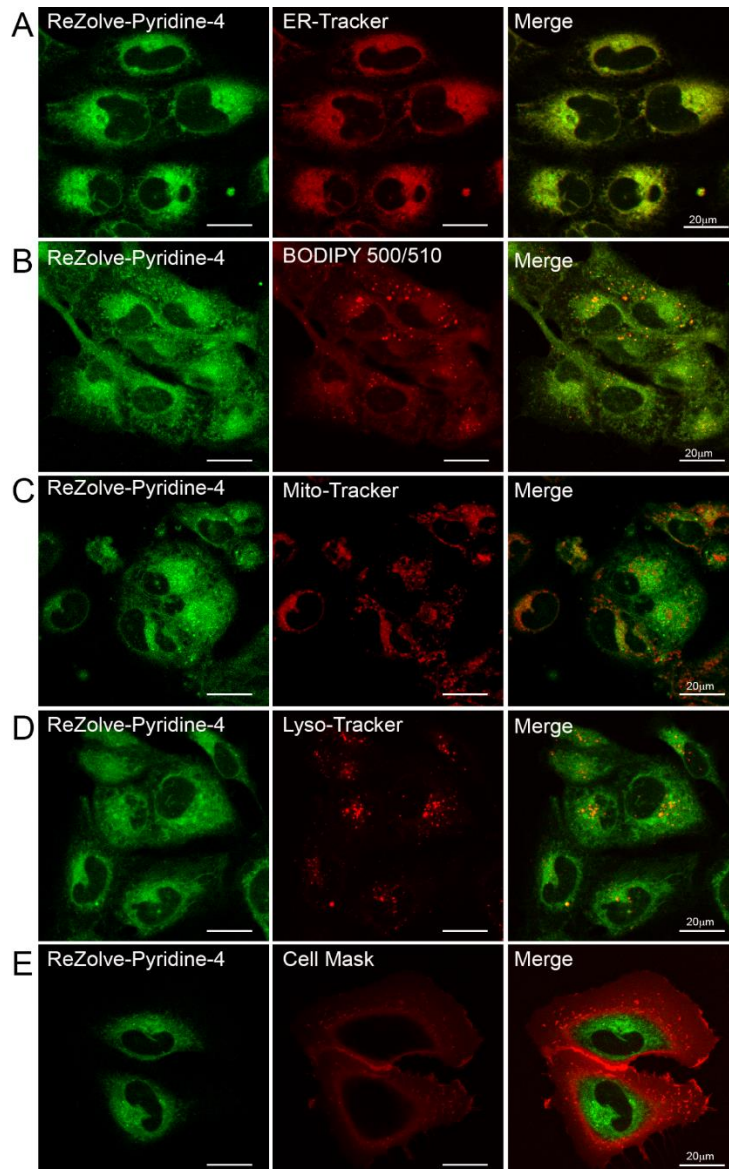
407



409

410 **Figure 1. ReZolve-ER™ does not photobleach when expose to high laser power.** (A-C)  
411 *Confocal micrographs of PNT2 cells incubated with ReZolve-ER™ for 0 min (A), 15 min (B)*  
412 *or 29 min (C). Overlay shows the regions of interest from which emissions intensity was*  
413 *measured. (D) Scatter plot showing average emission intensity (au) of ReZolve-ER™ stained*  
414 *cells from regions of interest indicated. Images collect with 403 nm excitation set to laser*  
415 *power 10, a scan rate of 0.22 s (give a total of 448 scans over 29.33 min) and a pixel dwell*  
416 *time of 0.22 ms.*

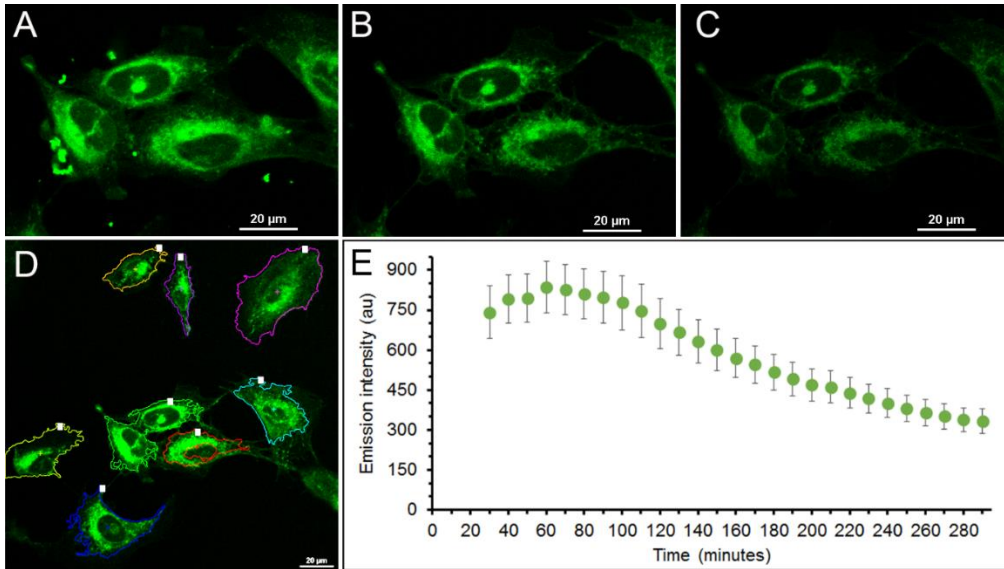
417



418

419 **Figure 2. ReZolve-ER<sup>TM</sup> subcellular localisation.** Confocal micrographs showing PNT2  
 420 cells incubated with ReZolve-ER<sup>TM</sup> (green) and counter stained with (A) ER-Tracker<sup>®</sup> for the  
 421 labelling of ER (red), (B) MitoTracker<sup>®</sup> for the labelling of mitochondria (red), (C)  
 422 LysoTracker<sup>®</sup> for the labelling of lysosomes/acidic compartments (red), and (D) CellMask<sup>TM</sup>  
 423 for the labelling of the plasma membrane (red).

424

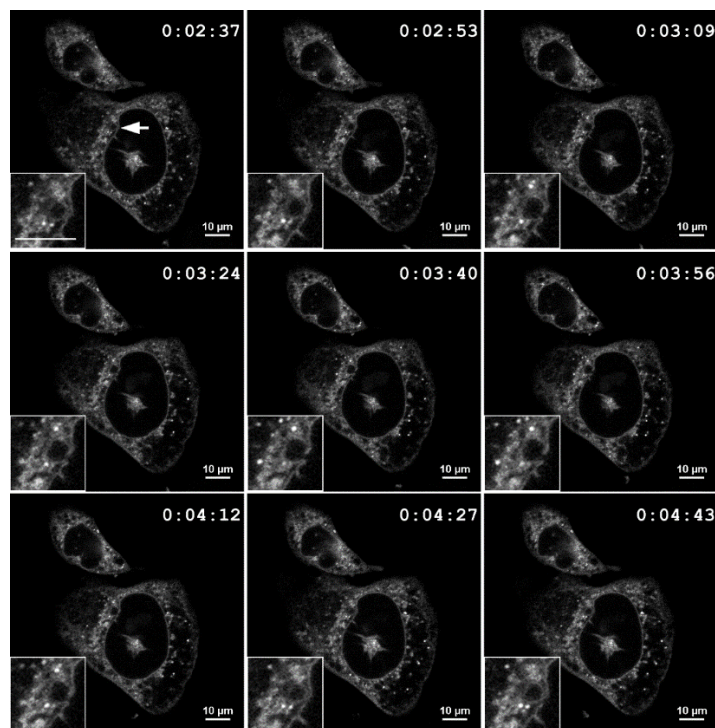


425

426 **Figure 3. ReZolve-ER™ localisation is unchanged over time.**

427 (A-D) Confocal micrographs of PNT2 cell incubated with ReZolve-ER™. Images taken at 20  
 428 min (A), 140 min (B) and 290 min (C) incubation time points. (D) Shows a dot plot of  
 429 emissions intensity over time. (E) Histogram of cell viability measured by an MTS assay in  
 430 response to incubation with ReZolve-ER™ (Re-ER) at 50 μM for 1 h, 4 h, 7 h or 24 h, when  
 431 compared to a negative control of 50% DMSO in culture media (-ive control), a positive  
 432 control of cells will full media (+ive control), and time point controls (control) in which cells  
 433 were expose to 0.5% DMSO for 1 h, 4 h, 7 h or 24 h. \* indicates a significant difference  
 434 between the negative control and all other treatment conditions, \*\* indicates significant  
 435 difference between indicated groups.

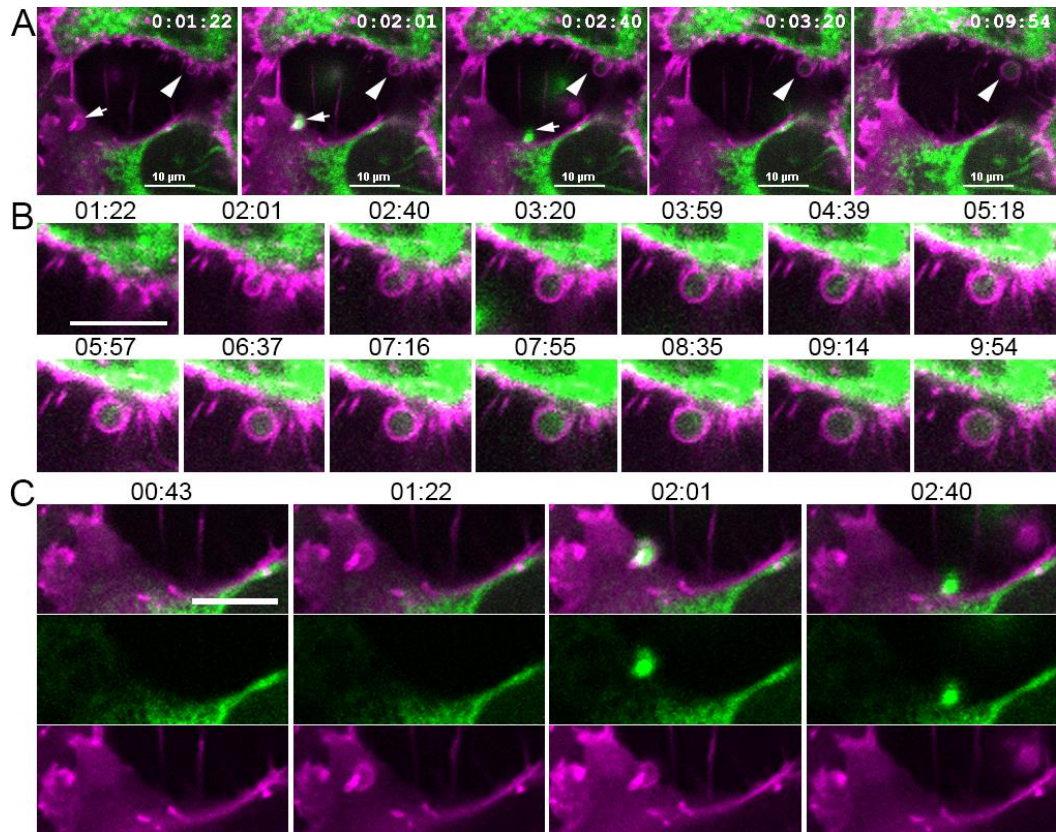
436



437

438 **Figure 4. Time lapse confocal imaging of ReZolve-ER<sup>TM</sup> in PNT2 cells.** Time of image  
 439 capture is indicated in the right hand corner of each frame; and represents the last five  
 440 minutes in a set of three consecutive time courses (i.e. total 15 min). Scale bar = 10  $\mu$ m.  
 441 Enlarged panel shows nuclear phagosome ( $\sim 3 \mu$ m) forming over the time course and intense  
 442 small ( $< 0.5 \mu$ m) vesicular staining.

443



444

445 **Figure 5. ReZolve-ER<sup>TM</sup> imaging of vesicle release from the cell surface.** Time lapse  
 446 confocal micrographs showing PNT2 cells stained with ReZolve-ER<sup>TM</sup> (green in A, B and C),  
 447 counterstained with Cell Mask (purple in A, B and C). (A) Two vesicle release events were  
 448 captured, arrow head indicated cross-section of budding vesicle forming which is enlarged in  
 449 panel B; arrow indicates budding event at the cell surface which is enlarged in panel C. Time  
 450 of capture is indicated in the right hand corner of each frame (A) or above each frame (B and  
 451 C). Scale bar = 10  $\mu$ m.

452